UDK 621.77:620.193:67.017:669.721.5
Original scientific article/Izvirni znanstveni članek

ISSN 1580-2949
MTAEC9, 55(4)525(2021)

INFLUENCE OF A PREFABRICATED-CROWN ROLLING PROCESS ON THE CORROSION BEHAVIOUR OF AZ31 MAGNESIUM ALLOY

VPLIV PROCESA VALJANJA KONVEKSNIH PREIZKUŠANCEV IZ MAGNEZIJEVE ZLITINE AZ31 NA NJENE KOROZIJSKE LASTNOSTI

Zhiquan Huang[1,2], Jinchao Zou[1,2*], Junpeng Wang[1,2], Yanjie Pei[1,2], Renyao Huang[1,2], Guowei Yang[3]

[1]Heavy Machinery Engineering Research Center of the Ministry of Education, Taiyuan University of Science and Technology, Taiyuan 030024, China
[2]School of Mechanical Engineering, Taiyuan University of Technology, Taiyuan 030024, China
[3]Gansu Construction Equipment Manufacturing Co., Ltd.

Prejem rokopisa – received: 2020-11-29; sprejem za objavo – accepted for publication: 2021-03-30

doi:10.17222/mit.2020.219

The present study aims to investigate the effect of a prefabricated-crown rolling process on the corrosion characteristic of the AZ31 magnesium alloy. Specimens made of the AZ31 alloy were rolled under various crown conditions, and their microstructure evolution and corrosion behavior were analyzed. The corrosion behavior was studied using potentiodynamic polarization and electrochemical impedance spectroscopy (EIS). The results showed that the corrosion-current density of the AZ31 alloy with a side pressure of 37.5 % of the plate thickness of the precast convexity decreased from 3.79×10^{-6} A/cm^2 to 1.80×10^{-6} A/cm^2, and the difference between the edge and the middle of the AZ31 alloy was shortened from 2.05×10^{-6} A/cm^2 to 1.14×10^{-6} A/cm^2. The charge-transfer resistance also increased from 507.1 Ω·cm^2 to 581.2 Ω·cm^2. The improvement in the corrosion resistance is a result of the more stable corrosion products and microstructure refinement formed after the prefabricated-crown rolling process.

Keywords: AZ31 magnesium alloy, prefabricated crown, rolling, corrosion, polarization

Namen študije je raziskati učinek valjanja konveksnih preizkušancev na korozijo, značilno za magnezijevo zlitino AZ31. Vzorci iz zlitine AZ31 so bili valjani pod različnimi pogoji konveksnosti preizkušancev, analiziran pa je bil razvoj njihove strukture in njihovo korozijsko obnašanje. Korozijsko obnašanje so preučevali s potenciodinamično polarizacijo in spektroskopijo elektrokemične impedance (EIS). Rezultati so pokazali, da se je gostota korozijskega toka zlitine AZ31 z bočnim tlakom 37,5 % debeline plošče predulitkov zmanjšala s $3{,}79 \times 10^{-6}$ A/cm^2 na $1{,}80 \times 10^{-6}$ A/cm^2, razlika med robom in sredino zlitine AZ31 pa se je zmanjšala z $2{,}05 \times 10^{-6}$ A/cm^2 na $1{,}14 \times 10^{-6}$ A/cm^2. Tudi upornost prenosa naboja se je povečala s 507,1 Ω·cm^2 na 581,2 Ω·cm^2. Izboljšanje odpornosti proti koroziji je posledica stabilnejših korozijskih produktov in izboljšane mikrostrukture nastale med izbranim načinom valjanja preizkušancev.

Ključne besede: magnezijeva zlitina AZ31, predizdelani preizkušanci konveksne oblike, valjanje, korozija, polarizacija

1 INTRODUCTION

A magnesium alloy is characterized by a low density and high specific strength, and has a wide application prospect in the lightweight-engineering fields such as aerospace and new-energy vehicles. It is considered as a "third-generation" metal structural material.[1–3] However, activation and corrosion of a magnesium alloy are very easy to occur, seriously affecting the stability of the magnesium alloy and being one of the reasons for a restriction of its engineering application.[4–6] The results show that a microstructure refinement can effectively improve the corrosion resistance of magnesium and its alloys, and large deformation processing is one of the most effective methods for the metal-grain refinement.[7–9]

Our group, studying magnesium-alloy rolling edge cracks found that the stress and strain distribution at the edge of a magnesium plate can be effectively changed, so that the edge and middle metal flow almost at the same time, which is conducive to the reduction of the edge damage of the magnesium plate.[10] However, the corrosion behavior of a magnesium alloy rolled with prefabricated-crown rolling was not reported. The corrosion behavior of magnesium alloys is related to many factors, such as microstructure, phase composition, alloy composition, working environment and the performance of the forming oxide film in an aqueous solution.[11–13] At present, prefabricated-crown rolling is only used to control the shape and edge crack damage of a magnesium alloy plate. It is not clear whether there is a genetic effect on the corrosion behavior of a magnesium alloy and how to influence it. Therefore, the main purpose of this study is to investigate how the microstructure of an AZ31 strip prepared under different convexity conditions affects the corrosion behavior.

*Corresponding author's e-mail:
Zou517375834@163.com (Zou Jinchao)

2 EXPERIMENTAL PART

2.1 Material preparation

Commercial AZ31 magnesium alloy ingots were used as the base material and prepared into prefabricated convex samples for a rolling experiment with a wire-cut electric-discharge machine. The basic thickness of the samples was 10 mm and the unilateral prefabricated convex dimensions were (0, 0.5, 0.75, 1) mm, respectively. In the previous research on the side-crack control of magnesium alloy rolling, the research group found that it was important for the side pressure to be lower than the initial thickness of the slab, and the best effect was achieved when the side pressure was 37.5 % of the plate thickness.[11] Therefore, this experiment was focused only on magnesium-alloy plates with a unilateral prefabricated convexity of 0 mm (plate) and 0.75 mm; the final shape and size are shown in **Figure 1**. The ingots were homogenized at 350 °C for 2 h, and then a single-pass rolling experiment was carried out with a double high rolling mill. The specific rolling parameters were as follows: the rolling temperature was 350 °C, the rolling speed was 0.1 m/s and the rolling volume was 35 %.

2.2 Corrosion tests

Corrosion-test samples were extracted by wire cutting from the middle and edge of the sheet after rolling. The samples were exposed to a 3.5 % sodium chloride solution at room temperature. Electrochemical tests were carried out on a PARSTAT 4000 electrochemical workstation with a three-electrode system. The sample for prefabricated-crown rolling was used as the working electrode, the platinum plate as the auxiliary electrode and the saturated calomel electrode (SCE) as the reference electrode. One end of the sample was welded with wires and sealed with epoxy resin, leaving only a working area of 1 cm^2. The frequency range from 10^5 Hz to 0.1 Hz was measured at a disturbance voltage amplitude of 5 mV. The Zsimpwin software was used to analyze and fit the measured experimental data. The scanning potential range of the dynamic potential polarization test was –0.3 V – +0.4 V, and the scanning rate was 3 mV/s. The experimental data were fitted by the Cview software, and relevant parameters such as corrosion potential, corrosion-current density, corrosion rate and Tafel slope were obtained.

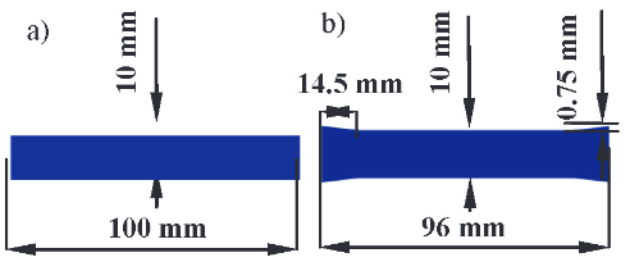

Figure 1: Cross-sectional shape of: a) a flat plate, b) a prefabricated plate with a convexity 0.75 mm

2.3 Microscopic measurements

Metallographic samples were extracted from the rolled plate and prefabricated-crown samples; they were polished step by step with 400#, 600#, 800#, 1200# and 1600# sandpaper. The samples were washed with absolute ethanol and then polished with a polishing machine. The polished samples were eroded with a corrosive mixture of 5 g picric acid, 100 mL ethanol, 5 mL acetic acid and 10 mL distilled water. They were scanned with a metallographic microscope, equipped with an energy spectrometer (EDS; INCA, Oxford Instruments) and an electron microscope (SEM; JSF-6700F) to observe the grains, grain boundaries and intergranular precipitates of the AZ31 magnesium alloy.

3 RESULTS AND DISCUSSION

3.1 Potentiodynamic-polarization curve

Figure 2 shows the polarization curves of the rolled prefabricated-crown (PC) plate and flat-plate samples in the 3.5 % NaCl solution. It can be seen from **Figure 2** that the cathodic-polarization curves of the four samples are basically the same, while the anodic-polarization curves show a similar phenomenon of self-passivation. Both at the edges and in the middle, the corrosion potential of the prefabricated-crown samples was positively shifted, and a higher corrosion potential indicated a lower corrosion tendency.[14] The corrosion-current density is inversely proportional to the corrosion resistance of the material. The smaller the corrosion current, the stronger is the corrosion resistance.[15–17]

The electrochemical data calculated with the Tafel extrapolation method are shown in **Table 1**. It can be seen that the corrosion current of the sample with the prefabricated crown of 0.75 mm is smaller than that of

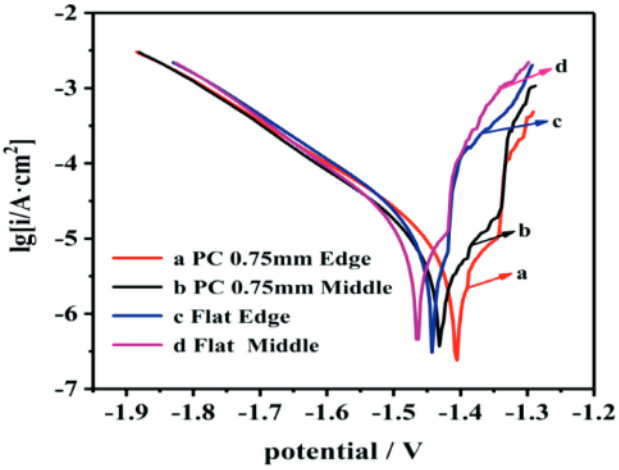

Figure 2: Polarization curves of the rolled prefabricated crown (PC) and flat-plate samples in the 3.5 % NaCl solution

the flat plate, regardless of the position, the edge or the middle. The difference in the corrosion-current density between the edge and the middle of the sample with the prefabricated crown of 0.75 mm is 1.14×10^{-6} A/cm^2, while the difference for the flat specimen is 2.05×10^{-6} A/cm^2, which is nearly twice shorter. It can be seen that the AZ31 magnesium alloy with the prefabricated crown of 0.75 mm does not only improve the overall corrosion resistance, but also reduces the difference in the corrosion resistance between the edge and the middle of the plate.

Table 1: Electrochemical data of all the samples immersed in the 3.5 % NaCl solution calculated with the Tafel extrapolation method

Sample code	E_{corr} (V)	I_{corr} (A/cm^2)
PC 0.75 mm edge	–1.40	2.94×10^{-6}
PC 0.75 mm middle	–1.42	1.80×10^{-6}
Flat edge	–1.44	5.84×10^{-6}
Flat middle	–1.46	3.79×10^{-6}

3.2 Electrochemical-impedance measurements

The electrochemical impedance spectra (EIS) curves of the samples of the rolled flat plate and the prefabricated-crown AZ31 magnesium alloy plate in the 3.5 % sodium chloride solution are shown in **Figure 3.** In this figure, A and B represent the edge and the middle of the specimen with a prefabricated crown of 0.75 mm, while C and D represent the edge and the middle of the flat-plate specimen, respectively. The Nyquist diagram (**Figure 3a**) of the prefabricated-crown sample after rolling shows two time constants; four samples are composed of a high-frequency capacitive-reactance arc and a low-frequency inductive-reactance arc. The capacitive-reactance arc in the high-frequency region is related to the electric double-layer capacitance and the reaction-transfer resistance. Due to the existence of the frequency-dispersion effect, the capacitive-reactance arc is not a perfect semicircle. Generally, the diameter of a capacitive loop is associated with the charge-transfer resistance, which is proportional to the corrosion resistance of the electrode material in the test solution.[18] The low-frequency-induced reactance is caused by pitting corrosion or a chemical reaction of magnesium ions with water and the corrosion products in the area without a film covering on the sample surface.[19] As can be seen from the coordinate values of the impedance spectrum in **Figure 3a**, the diameter of the sample with the prefabricated crown of 0.75 mm is larger than that of the flat plate, namely, A > C, B > D. That is, the sample with the prefabricated crown of 0.75 mm has a higher corrosion resistance, and the test results are consistent with the previous discussion.

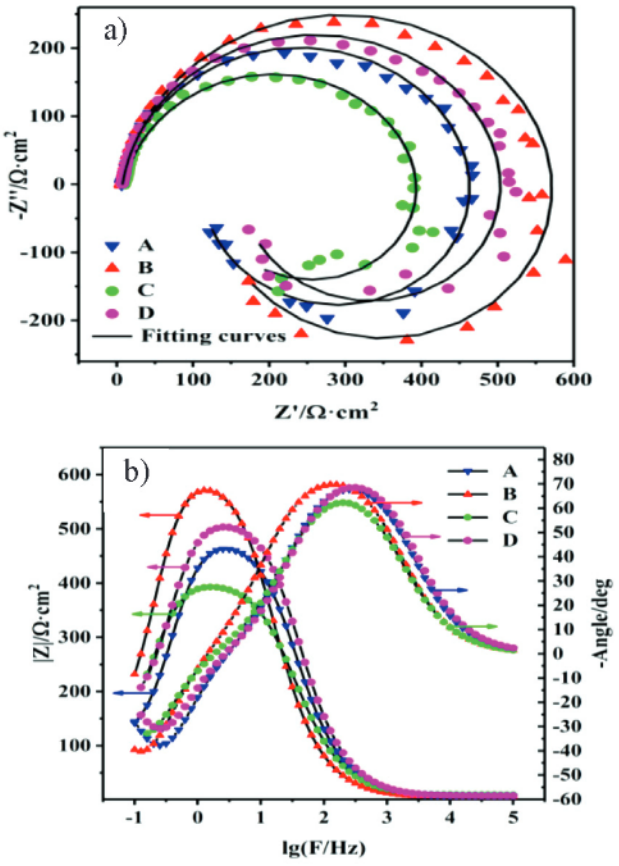

Figure 3: Electrochemical impedance spectrum (EIS) curves of the samples of the rolled flat plate and prefabricated-crown AZ31 magnesium alloy plate in the 3.5 % sodium chloride solution: a) Nyquist diagram and the fitting curve, b) fitting curve of the Bode graph

The electric equivalent-circuit diagram of the samples of the flat plate and the prefabricated-crown magnesium alloy is shown in **Figure 4**, where R_s is the solution resistance, R_t is the charge-transfer resistance, and C is the interface capacitance of the double electric layer at the interface between the electrode and the solution; the constant phase-angle element Q is often used to replace the capacitance.[20] The inductive-reactance arc in the low-frequency region represents the desorption of the corrosion products, usually represented by inductance L and resistance R_l in a series.

The impedance data are fitted to the electrical equivalent circuit by the Zsimpwin software, and the results are shown in **Table 2**. Due to the good electrical conductivity of the sodium chloride solution, the R_S values of the four samples were close to each other and relatively small, while the R_t values of the sample with the prefabricated crown of 0.75 mm were significantly higher than those of the flat plate. The charge-transfer resistance (R_t)

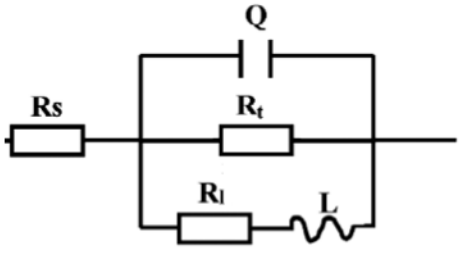

Figure 4: Equivalent circuit of the fitting impedance spectrum

is proportional to its corrosion resistance.[21] This also means that the corrosion resistance of the prefabricated-crown specimen is improved. The n value is equivalent to the dispersion factor; if it is close to 1, it means that the electrode surface is smooth and flat, leading to the formation of a dense oxide film.[22] The n value of the sample with the prefabricated crown of 0.75 mm is close to that of the other sample, which means that the density of MgO at the edge and the middle is basically the same. The gap between the corrosion-resistance values for the middle and the edge of the prefabricated-crown magnesium alloy is reduced after rolling. The reason for it is the fact that the sliding deformation of the plate in the middle and front of the edge is synchronized during rolling, the tensile stress is obviously weakened, and the tensile-stress range before and after the deformation zone is greatly reduced.[11] This conclusion is consistent with the previous tests.

3.3 Microstructure

The microstructures of the edge and middle parts of the rolled flat plate and prefabricated-crown plate are shown in **Figure 5**. The microstructures of the flat magnesium-alloy specimens (**Figures 5c** and 5**d**) show an uneven distribution of coarse and fine grains, while the grains of the prefabricated crown of 0.75 mm (**Figures 5a** and 5**b**) are relatively uniformly distributed. This is because the sample's prefabricated edge crown can effectively change the stress and strain distribution at the edge of the magnesium plate during the rolling process, so that the metal at the edge and middle parts can flow as synchronously as possible; the plate tends to be uniformly deformed and the grains are uniformly distributed.[11,23] As shown in **Figure 5a**, the edge grains are refined, and both columnar and equiaxial grains are abundant. This is due to the dynamic recrystallization of the prefabricated edge-crown sample during rolling, resulting in the appearance of some equiaxial grains.[24] As the three-dimensional stress in the middle of the plate is significantly reduced after the prefabricated edge crown, resulting in a low grain-refinement degree in the middle of the plate, the size of the middle grains is increased (**Figure 5b**). It is for this reason that the grain gap between the edge and the middle of the prefabricated-crown plate is reduced, and the grain size of the whole plate tends to be the consistent.

3.4 Characterization of the corrosion layer

Figure 6 shows the surface morphology of the four samples with the edge and middle of the prefabricated crown of 0.75 mm and the flat plate after immersion in the 3.5 % NaCl solution for 24 h. The corrosion degree

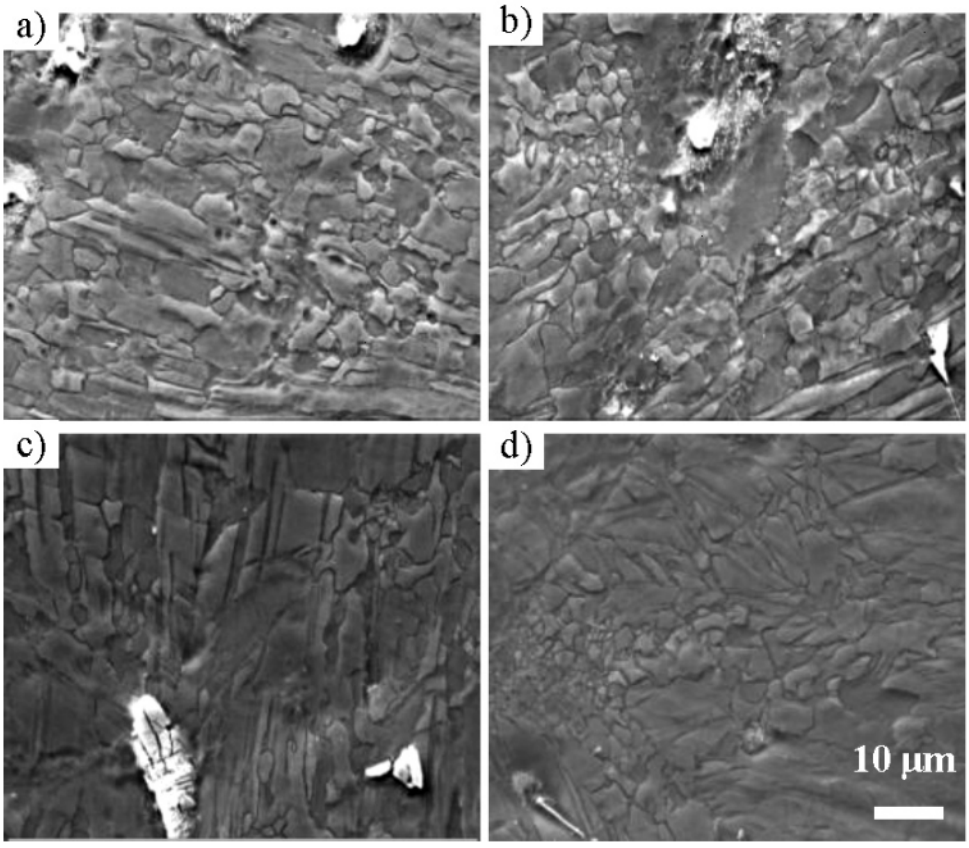

Figure 5: Microstructures of flat-plate and prefabricated-crown samples after rolling: a) and b) represent the edge and middle of the prefabricated 0.75 mm sample, respectively, c) and d) represent the edge and middle of the flat sample, respectively

Table 2: Electrochemical parameters obtained with electrochemical-impedance-spectroscopy fitting

Sample code	R_s/Ω·cm^2	C/Ω^{-1}·cm^{-2}·s^n	n	R_t/Ω·cm^2	L/Ω·cm^2·s	R_l/Ω·cm^2
PC 0.75 mm edge	7.19	2.13×10^{-6}	0.9049	467.7	183.3	135.8
PC 0.75 mm central	6.33	3.62×10^{-6}	0.904	581.2	418.5	148.6
Flat edge	9.70	3.04×10^{-6}	0.8797	391.9	330.6	146.6
Flat central	7.47	1.73×10^{-6}	0.9103	507.1	251.3	224.6

for the four samples was arranged in the order from large to small: the edge of the flat plate > the edge of the prefabricated-crown 0.75 mm plate > the middle of the flat plate > the middle of the prefabricated-crown 0.75 mm plate. The surface of the sample at the edge of the flat plate is completely corroded, the film is thick and loose, with large cracks and a flaky structure (**Figure 6c**). The solution penetrates into the magnesium-alloy matrix through the cracks, and may aggravate the corrosion. However, the surface of the sample with the prefabricated crown of 0.75 mm shows cracks and surface peeling off, but the intact area is large. Compared with the sample from the middle of the flat plate (**Figure 6d**), the surface of the middle sample with the prefabricated crown of 0.75 mm (**Figure 6b**) shows a more uniform and dense corrosion layer with fewer cracks and discontinuities. The formed corrosion layer prevents the matrix from further contacts with the solution and plays a protective role.

The corrosion rate of a magnesium alloy is usually related to the size and uniformity of the grains. Especially when the 3.5 % NaCl solution is used as the corrosive medium, the size of grains affects the chemical activity and energy of the material.[25,26] Zheng et al.[27] studied the effect of the grain size on the electrochemical performance of pure magnesium. Alloy stacking faults and defects usually affect the reaction process of the cathode, which may increase the volume fraction of the effective cathode, thus affecting the corrosion rate of the magnesium alloy. A large-size microstructure and residual stresses have negative effects on the corrosion behavior, while grain refinement has positive effects on the corrosion behavior.[28,29] Therefore, the improvement in the corrosion resistance of the AZ31 alloy after the prefabrication of the edge crown is mainly due to the refinement of Mg grains and a uniform distribution of micro-components. Because of the uniform distribution of the microstructure in the magnesium alloy, the difference

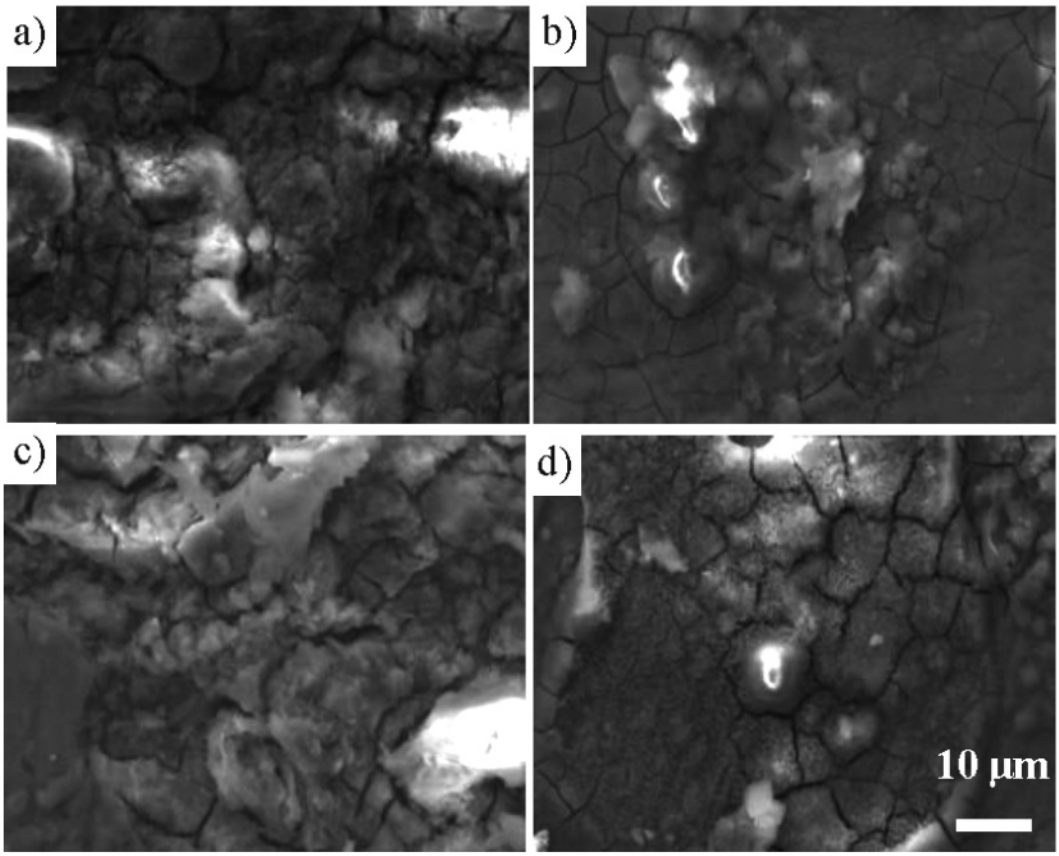

Figure 6: Surface corrosion morphology of the sample in the 3.5 % NaCl solution for 24 h: a) and b) show the edge and middle of the prefabricated convexity of 0.75 mm, respectively, c) and d) show the edge and middle of the flat plate, respectively

in the corrosion properties between the edge and middle parts of the magnesium alloy is reduced.

4 CONCLUSIONS

1) According to the lower corrosion-current density from the polarization experiment and the higher charge-transfer resistance obtained with electrochemical impedance spectroscopy (EIS), the corrosion-current density in the middle of the flat-plate sample is 3.79×10^{-6} A/cm^2, and the corrosion-current density in the middle of the sample with the prefabricated crown of 0.75 mm is 1.80×10^{-6} A/cm^2. The charge-transfer resistance in the middle of the flat-plate sample is 507.1 Ω·cm^2, and the charge-transfer resistance in the middle of the sample with the prefabricated crown of 0.75 mm is 581.2 Ω·cm^2; therefore, the rolled sample with the prefabricated crown of 0.75 mm has better corrosion resistance.

2) According to the microstructure and corrosion appearance, dense corrosion products, a grain refinement and a uniform distribution can effectively improve the corrosion resistance of magnesium-alloy plates. The difference in the corrosion-current density between the edge and the middle of the flat magnesium-alloy sample is 2.05×10^{-6} A/cm^2, while that for the magnesium-alloy sample with the prefabricated crown of 0.75 mm is only 1.14×10^{-6} A/cm^2. After the edge crown is prefabricated, the corrosion-resistance gap between the edge and middle can be effectively reduced and the corrosion-resistance uniformity of the plate can be enhanced.

Acknowledgment

This research was funded by the National Key Research and Development Plan (2018YFA0707301), National Natural Science Foundation of China (52075357) and Shanxi Provincial Science and Technology Major Special Project (20181102016).

5 REFERENCES

[1] C. Q. Li, Z. R. Zeng, L. Y. Sheng, X. B. Chen, Effect of volume fraction of LPSO phases on corrosion and mechanical properties of Mg-Zn-Y alloys, Mater. Design, 121 (**2017**), 430–441, doi:10.1016/j.matdes. 2017.02.078

[2] L. B. Peral, A. Zafra, S. Bagherifard, M. Guagliano, I. Fernández-Pariente, Effect of warm shot peening treatments on surface properties and corrosion behavior of AZ31 magnesium alloy, Surf. Coat. Tech., 401 (**2020**), 126285, doi:10.1016/j.surfcoat.2020.126285

[3] Y. Zhi, X. Hong, H. J. Hu, D. F. Zhang, Z. W. Ou, Y. N. Gou, L. J. Chai, Improving the corrosion resistance of the AZ61 mangnesium alloy with a homogenization treatment before the extrusion-shear process, Mater. Tehnol., 52 (**2018**) 6, 803–808, doi:10.17222/mit.2018.102

[4] H. L. Liu, Z. P. Tong, W. F. Zhou, Y. Yang, J. F. Jiao, X. D. Ren, Improving electrochemical corrosion properties of AZ31 magnesium alloy via phosphate conversion with laser shock peening pretreatment, J. Alloy Compd., 846 (**2020**), 155837, doi:10.1016/j.jallcom.2020.155837

[5] L. Sun, Y. Ma, J. S. Wang, L. Y. An, S. Wang, Z. Y. Wang, Preparation and corrosion resistance of hybrid coatings formed by PEN/C plus PEO on AZ91D magnesium alloys, Surf. Coat. Tech., 390 (**2020**), 125661, doi:10.1016/j.surfcoat.2020.125661

[6] G. Barati Darband, M. Alifkhazraei, P. Hamghalam, N. Valizade, Plasma electrolytic oxidation of magnesium and its alloys: mechanism, properties and applications, J. Magnes. Alloys, 5 (**2017**), 74–132, doi:10.1016 /j.jma.2017.02.004

[7] S. Hamed, H. S. Mahmoud, A. Mohammad, A. Donya, S. Mohsen, Influence of friction stir processing conditions on corrosion behavior of AZ31B magnesium alloy, J. Magnes Alloys, 7 (**2019**), 605–616, doi:10.1016/j.jma.2019.11.004

[8] A. Onder, Effect of die parameters on the grain size, mechanical properties and fracture mechanism of extruded AZ31 magnesium alloys, Mat. Sci. Eng. A., 793 (**2020**), 139887, doi:10.1016/j.msea.2020.139887

[9] J. F. Deng, G. S. Huang, Y. C. Zhang, B. Wang, Electrochemical Performance of AZ31 Magnesium Alloy under Different Processing Conditions, Rare Metal Mat. Eng., 43 (**2014**), 316–321, doi:10.1016/S1875-5372(14)60066-7

[10] Z. Q. Huang, Q. X. Huang, J. C. Wei, L. F. Ma, D. Z. Wu, D. P. He, Inhibitory effects of prefabricated crown on edge crack of rolled AZ31 magnesium alloy plate, J. Mater. Process. Tech., 246 (**2017**), 85–92, doi: 10.1016/j.jmatprotec.2017.01.034

[11] J. L. Ma, Y. Zhang, M. S. Ma, C. H. Qin, F. Z. Ren, G. X. Wang, Corrosion and discharge performance of a magnesium aluminum eutectic alloy as anode for magnesium–air batteries, Corros. Sci., 170 (**2020**), 108695, doi:10.1016/j.corsci.2020.108695

[12] B. Mingo, M. Mohedano, C. Blawert, R. Delolmo, N. Hort, R. Arrabal, Role of Ca on the corrosion resistance of Mg-9Al and Mg-9Al-0.5Mn alloys, J. Alloy Compd., 811 (**2019**), 0925–8388, doi:10.1016 /j.jallcom.2019.151992

[13] T. X. Zheng, Y. B. Hu, S. W. Yang, Effect of grain size on the electrochemical behavior of pure magnesium anode, J. Magnes. Alloys, 5 (**2017**), 404–411, doi:10.1016/j.jma.2017.09.003

[14] H. Liu, Y. Yan, X. H. Wu, H. J. Fang, X. Chu, J. F. Huang, J. X. Zhang, J. M. Song, K. Yu, Effects of Al and Sn on microstructure, corrosion behavior and electrochemical performance of Mg-Al-based anodes for magnesium-air batteries, J. Alloys Compd., (**2020**), 157755, doi:10.1016/j.jallcom.2020.157755

[15] X. R. Chen, Y. H. Jia, Q. C. Le, H. N. Wang, X. Zhou, F. X. Yu, A. Atrens, Discharge properties and electrochemical behaviors of AZ80-La-Gd magnesium anode for Mg-air battery, J. Magnes. Alloys, (**2020**), doi:10.1016/j.jma.2020.07.008

[16] H. R. Tiyygura, H. Puliyalil, G. Filipic, K. Kumar, Y. B. Pottathara, R. Rudolf, Corrosion studies of plasma modified magnesium alloy in simulated body fluid (SBF) solutions, Surf. Coat. Tech., 385 (**2020**), 125434, doi:10.1016/j.surfcoat.2020.125434

[17] M. Hren, T. Kosec, A. Legat, V. Bokan-Bosiljkov, Corrosion performance of steel in blended cement pore solutions, Mater. Tehnol., 54 (**2020**) 3, 393–396, doi:10.17222/mit.2019.224

[18] L. A. Oliveira, R. M. Silva, A. C. Rodas, R. M. Souto, R. A. Antunes, Surface chemistry, film morphology, local electrochemical behavior and cytotoxic response of anodized AZ31B magnesium alloy, J. Mater. Res. Technol., 9 (**2020**), 14754–14770, doi:10.1016/j.jmrt.2020.10.063

[19] G. Baril, N. Pebere, The corrosion of pure magnesium in aerated and deaerated sodium sulphate solutions, Corros. Sci., 43 (**2001**), 471–484, doi:10.1016/S0010-938X(00)00095-0

[20] J. R. Li, Q. T. Jiang, H. Y. Sun, Y. T. Li, Effect of heat treatment on corrosion behavior of AZ63 magnesium alloy in 3.5 wt.% sodium chloride solution, Corros. Sci., 111 (**2016**), 288–301, doi:10.1016/j.corsci.2016.05.019

[21] F. L. Tong, X. Z. Chen, Q. Wang, S. H. Wei, W. Gao, Hypoeutectic Mg–Zn binary alloys as anode materials for magnesium-air batteries, J. Alloys Compd., (**2020**), 157579, doi:10.1016/j.jallcom.2020.157579

[22] Q. Liu, Q. X. Ma, G. Q. Chen, X. Cao, S. Zhang, J. L. Pan, G. Zhang, Q. Y. Shi, Enhanced corrosion resistance of AZ91 magnesium alloy through refinement and homogenization of surface microstructure by friction stir processing, Corros. Sci., 138 (**2018**), 284–296, doi:10.1016 /j.corsci.2018.04.028

[23] F. K. Ning, X. Zhou, Q. C. Le, X. Q. Li, Y. Li, Fracture and deformation characteristics of AZ31 magnesium alloy plate during tension rolling, Mater. Today Commun., 24 (**2020**), 101129, doi:10.1016/j.mtcomm. 2020.101129

[24] L. L. Catorceno, H. F. Abreu, A. F. Padilha, Effects of cold and warm cross-rolling on microstructure and texture evolution of AZ31B magnesium alloy sheet, J. Magnes Alloys, 6 (**2018**), 121–133, doi:10.1016/j.jma.2018.04.004

[25] J. S. Liao, M. Hotta, N. Yamamoto, Corrosion behavior of fine-grained AZ31B magnesium alloy, Corros. Sci., 61 (**2012**), 208–214, doi:10.1016/j.corsci.2012.04.03

[26] N. G. Wang, Y. C. Mu, W. H. Xiong, J. C. Zhang, Q. Li, Z. C. Shi, Effect of crystallographic orientation on the discharge and corrosion behaviour of AP65 magnesium alloy anodes, Corros. Sci., 144 (**2018**), 107–126, doi:10.1016/j.corsci.2018.08.003

[27] T. X. Zheng, Y. B. Hu, S. W. Yang, Effect of grain size on the electrochemical behavior of pure magnesium anode, J. Magnes. Alloys, 5 (**2017**), 404-411, doi:10.1016/j.jma.2017.09.003

[28] B. J. Wang, K. Xu, D. K. Xu, X. Cai, Y. X. Qiao, L. Y. Sheng, C. Anisotropic, corrosion behavior of hot-rolled Mg-8 wt.% Li alloy, J. Mater. Sci. Technol., 53 (**2020**), 102–111, doi:10.1016/j.jmst.2020.04.029

[29] F. J. Liu, Y. Ji, Z. Y. Sun, J. B. Liu, Y. X. Bai, Z. K. Shen, Enhancing corrosion resistance and mechanical properties of AZ31 magnesium alloy by friction stir processing with the same speed ratio, J. Alloys Compd., 829 (**2020**), 154452, doi:10.1016/j.jallcom.2020.154452